PREPARATION AND CHARACTERIZATION OF A NEW NANOCOMPOSITE SYSTEM BASED ON DENDRIMER/CARBON NANOTUBE PAIR

LAURA RICCO[1], JENNY ALONGI[1], LUCA VALENTINI[2], ILARIA ARMENTANO[2], ALBERTO MARIANI[3], SAVERIO RUSSO[1], JOSE M. KENNY[2]

[1]*Department of Chemistry and Industrial Chemistry, University of Genova and INSTM Local Unit, Via Dodecaneso 31, 16146 Genova, Italy*
[2]*Materials Science and Technology Centre, University of Perugia and INSTM Local Unit, Loc. Pentima Bassa, 05100 Terni, Italy*
[3]*Department of Chemistry, University of Sassari and INSTM Local Unit, Via Vienna 2, 07100 Sassari, Italy*

Received 21 July 2005; accepted 20 September 2005

Abstract
A new nanocomposite formed by single walled carbon nanotubes (SWNTs) and a semiconducting dendrimer with aromatic end groups (PAMAMC) has been prepared and investigated. The good dispersion of SWNTs in PAMAMC matrix has been promoted by sonication in a suitable medium, e.g. N,N-dimethylformamide (DMF). The product obtained has been characterized by SEM and TEM microscopies in order to verify the formation of a nanocomposite system, while UV-Vis and Raman spectroscopies have been considered for investigation on type and level of non-covalent interaction between PAMAMC and SWNT. Finally, in relation to potential photoelectrical properties of the system based on donor (PAMAMC) and acceptor (SWNT) pair, analysis of PAMAMC/SWNT systems exposed to UV light shows that conductivity increases and that a possible transport mechanism is governed by the formation of a charge transfer complex.

1. Introduction

Since their discovery in 1991 [1], carbon nanotubes have attracted much attention in various fields of nanoscience and nanotechnology [2-4]. Single walled carbon nanotubes are molecular wires that exhibit interesting structural, mechanical, electrical and electromechanical properties [5-7]. Various modifications of SWNTs by organic molecules have been performed; namely, both covalent [8-11] and non-covalent [12-25] sidewall functionalizations of carbon nanotubes with organic molecules have been performed, with the aims of emphasizing the above properties and finding new interesting applications in the nanotechnology field. The covalent functionalization of carbon nanotubes is often difficult and uncontrollable, and its efficiency largely depends on the concentration of defective sites in nanotube structure [26]. Moreover, covalent functionalization may locally destroy the sp^2 structure of SWNTs, thereby worsening their pristine mechanical and electronic properties. On the contrary, non-covalent functionalization seems a more friendly strategy to exploit SWNT properties. Many molecules, characterized by aromatic and/or conjugated structures, have shown to be suitable for this purpose, being able to interact with the sidewall surface of SWNTs thanks to their π-electron structure. Namely, small molecules as anthracene [25] and pyrene [13,22] derivatives, porphyrines [12] and higher molecular weight molecules like polyaniline [21] and polyphenylenevinylenes [20,23,24] have been successfully used.

In the present paper we have explored the possibility of combining SWNTs with an organic structure basically different from the ones mentioned above, i. e. a 3-D structure made of a dendrimer. The dendrimer (PAMAMC, Fig. 1) has been synthesized following Tomalia's group method [27] by peripherally modifying generation three of commercial amino-terminated PAMAM® (Sigma Aldrich), end-capped by 32 substituted naphthalene diimides. These latter, as dendrimer end groups, ensure the high level of π-bonds needed to interact non-covalently with carbon nanotubes. In addition, PAMAMC has interesting conducting properties, due to inter- and intra-molecular π-stacking links among its aromatic groups that perform a 3-D conducting network. We believe that this peculiarity should find suitable applications when PAMAMC and (1) is associated to carbon nanotubes to give rise to a donor-acceptor system.

2. Experimental Section

2.1 Materials

PAMAMC was a laboratory preparation synthesized by reacting the amino terminal groups of a generation

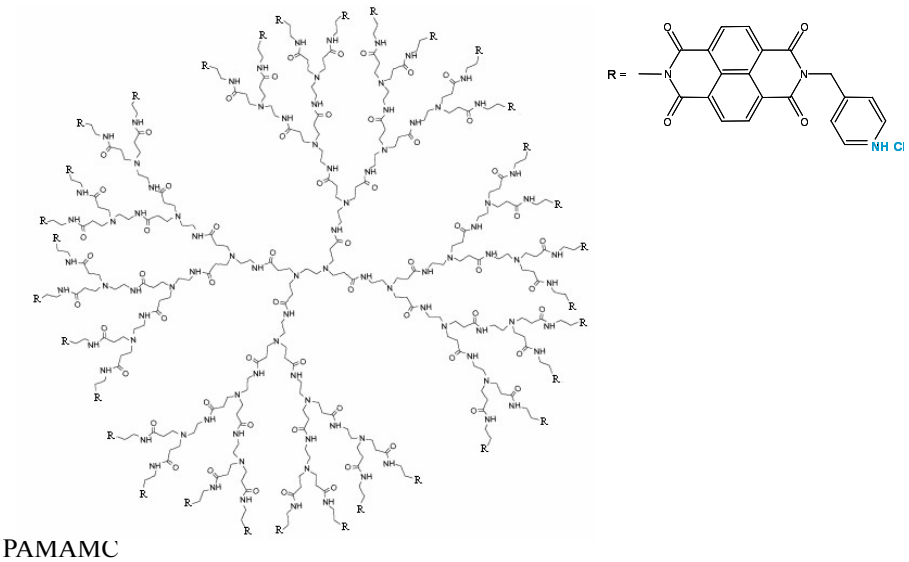

Fig. 1: Structure of PAMAMC

three PAMAM and (1), i.e. the 1,8-monoanhydride 4,5-monoimide of 1,4,5,8-naphthalene tetracarboxylic acid. The mono-substituted imide moiety is based on 4-(amino methyl)pyridine hydrochloride (Scheme 1). (1) was prepared in two steps following Scheme 2. DMAc is N,N-dimethylacetamide. Details on the synthesis of (1) and the reaction with PAMAM end groups are taken from [27].

SWNTs were obtained from CarboLex, Inc. and consisted of ≈ 50-70 vol% carbon as SWNTs, produced using the arc discharge method with a Ni-Y catalyst. Their characteristic diameter was in the range of 1.3-1.5 nm and most of them were embedded in bundles with a typical size of 7-12 nm. DMF (Aldrich) was used without further purification to prepare suspensions of SWNT/PAMAMC pairs.

2.2 Preparation of the nanocomposite

A typical procedure is as follows: PAMAMC was dissolved in DMF, SWNTs were added and submitted to sonication for two hours in a ultrasonic bath at room temperature. Samples characterized by different SWNT/PAMAMC ratios were prepared with the aim of investigating the non-covalent interactions between the two components of the system. Accordingly, PAMAMC samples combined with 1, 10, 20, 30 wt% of SWNTs were considered. For the sake of comparison, a neat sample of SWNTs and a neat sample of PAMAMC, both in DMF, were prepared following the same procedure.

2.3 Characterization

With the aims of both studying the level of mixing

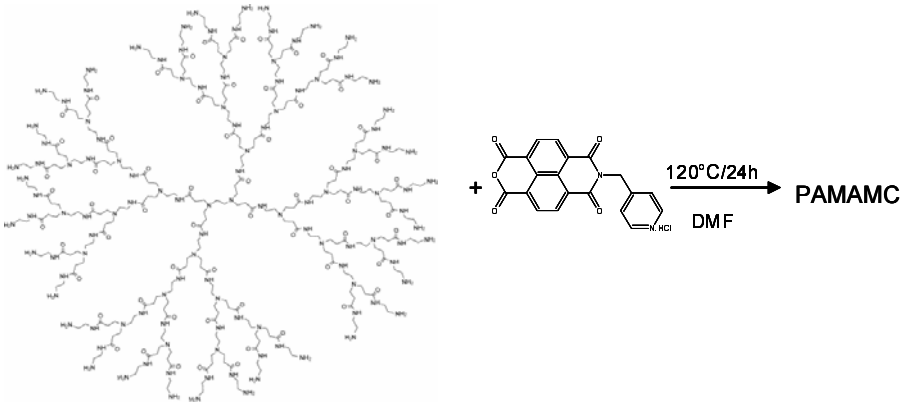

Scheme 1. Synthesis of PAMAMC from G3 PAMAM

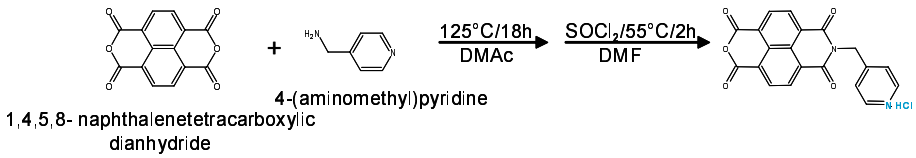

Scheme 2. Synthesis of the monoimide monoanhydride (1)

between nanotubes and dendrimer, and verifying the nanocomposite formation, electron microscopy was used. Transmission electron microscope measurements were performed on a Jeol Jem 2010, while scanning electron microscope measurements were carried out on a Leo Stereoscan 440. A Perkin-Elmer Lambda 9 UV spectrophotometer was used to monitor possible modifications of the PAMAMC structure as a consequence of the interactions with carbon nanotubes. The samples were analysed in the solid state as well as in solution. As far as the solid state analysis is concerned, a thin liquid film of their suspension in DMF was placed on glass supports by spin coating and dried under vacuum. The solutions were prepared by centrifugation of the suspensions followed by the removal of precipitate.

Raman spectroscopy was performed on powdered samples after DMF removal by vacuum distillation, in order to study possible shifts of nanotube typical peaks induced by PAMAMC after sonication. The apparatus was a Bruker RF100 provided with NdYAG laser (λ=1064 nm).

In order to check whether the presence of UV light leads to photoinduced conductivity changes into the SWNT/PAMAMC composite, electrical resistance was monitored for several on/off lighting cycles as a function of exposure to UV radiation. The electrical resistance of the film was measured in flowing air, using a volt-amperometric technique by a Keitley 236 multimeter fixing the temperature of the samples at 298 K. Samples for the electrical measurements were prepared by depositing a drop (1μl) of the solution of PAMAMC, naphthalenediimide and SWNT/PAMAMC dispersed in DMF, respectively, onto Pt electrical contacts that were allowed to dry in air for 24h. The electrical resistance of the film was measured in air.

3. Results & Discussion

At first, the suspension containing PAMAMC with 30 wt% of carbon nanotubes has been centrifuged in order to remove the insoluble fraction from the solution. The insoluble fraction has been found to be composed of carbon nanotubes and a part of PAMAMC not soluble in DMF. For the sake of comparison, also a neat sample of PAMAMC in DMF has been centrifuged to remove the dendrimer insoluble fraction. Although DMF is not able to completely solubilize the dendrimer, it has been chosen as diffusing medium for the process of sonication as the best of the media tested. Indeed, other solubility tests, carried out in dimethylsulfoxide, dichloromethane, chloroform, tetrahydrofuran, methanol, pyridine, N-methylpyrrolidone, acetonitrile, have given higher amounts of insoluble material. The limited solubility of PAMAMC in common organic solvents can be due to intermolecular π-stacking interactions among its peripheral aromatic groups. In addition, DMF has been preferred to other solvents on the basis of previous studies [28,29] aimed to find a suitable medium for solubilization/dispersion of SWNTs. As a result of these investigations, DMF and N-methylpyrrolidone have been found to be the best solvents both for generating stable dispersions of nanotubes, and for debundling their aggregates.

The clear soluble fractions obtained after centrifugation has been studied in order to evaluate whether dissolved PAMAMC is able to solubilize SWNTs by non-covalent interactions, as it occurs when aromatic molecules such as porphyrines [12], pyrenes [13,22], and conjugated polymers [20,23,24] are considered.

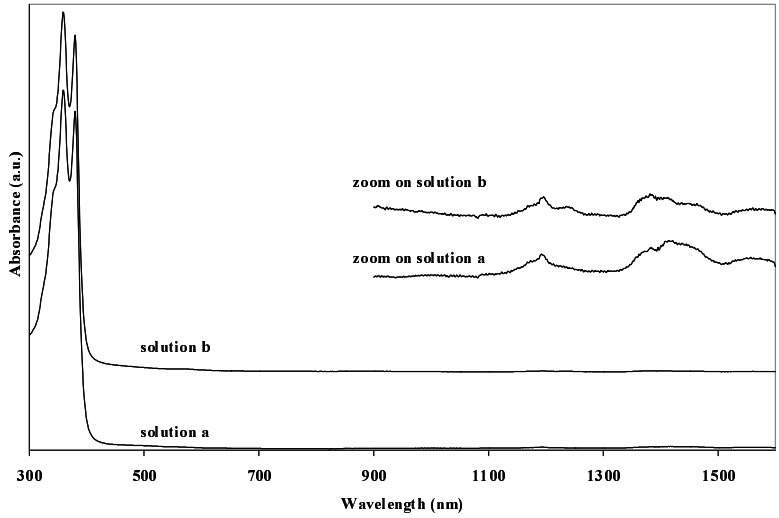

Fig 2: UV-Vis-NIR spectra of DMF soluble fractions of PAMAMC (solution a) and PAMAMC + 30wt% of SWNTs (solution b).

UV-Vis-NIR spectra of both pristine PAMAMC (solution *a*) and PAMAMC with 30wt% of SWNTs (solution *b*) were performed in the wavelength range between 300 and 1600 nm, in order to detect the absorbances coming from PAMAMC and to find the signals of carbon nanotubes. Spectra of the two solutions are compared in Fig.2, where the data are normalized to the main peak in the spectrum at 360 nm. PAMAMC shows two typical peaks at 360 and 380 nm due to the naphthalenediimide groups [30], while the typical signals of carbon nanotubes should appear in the NIR region of the spectrum. In presence of non-covalent interactions involving peripheral naphthalenediimides and SWNT in solution *b*, we should expect the following differences between the two spectra: i) a modification and/or a shift of solution *b* curve in comparison to solution *a* curve, in the range between 300 and 400 nm, and ii) the appearance of SWNT signals in the NIR region of the solution *b* spectrum. From the spectra of Fig.2, completely superimposed, it is evident that PAMAMC is not able to solubilize carbon nanotubes in DMF.

As a confirmation of this result, a drop of solution *b* has been placed on a freshly cleaved mica substrate and observed by a SEM microscope after solvent removal. Also in this case no presence of SWNTs has been noticed.

The above preliminary results do not rule out the chance of non-covalent interactions between PAMAMC and SWNTs, but push back the possibility of nanotube solubilization because of these interactions, when a diffusing medium such as DMF is used. In our opinion, this is mostly due to the limited solubility of the dendrimer in DMF.

As a consequence of these preliminary data, a detailed study of the whole system, including the insoluble fraction of PAMAMC and SWNTs, has been the following step of our research.

The stable suspensions prepared by sonication of PAMAMC with 0, 1, 10, 20, 30 wt% of carbon nanotubes in DMF have been placed on suitable supports and observed by SEM and TEM after solvent removal by evaporation. SEM and TEM micrographs of the composites containing 1wt% of carbon nanotubes are given in Figs. 3 and 4, respectively. SEM micrograph (Fig. 3) is centred on an isolated carbon nanotube and particles of PAMAMC surrounding it, and emphasizes the close interactions between the two components. Elemental analysis by x-ray energy-dispersive spectroscopy (EDS), limited to N atoms, allows differentiating the dendrimer from the nanotubes. The observation of the system in different areas reveals that isolated or bundled nanotubes are so well dispersed in the PAMAMC matrix to form a nanocomposite material.

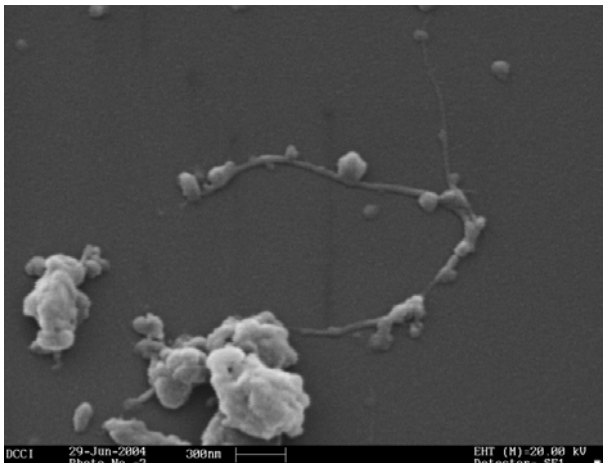

Fig. 3: SEM micrograph of the nanocomposite formed by PAMAMC + 1 wt% of SWNTs.

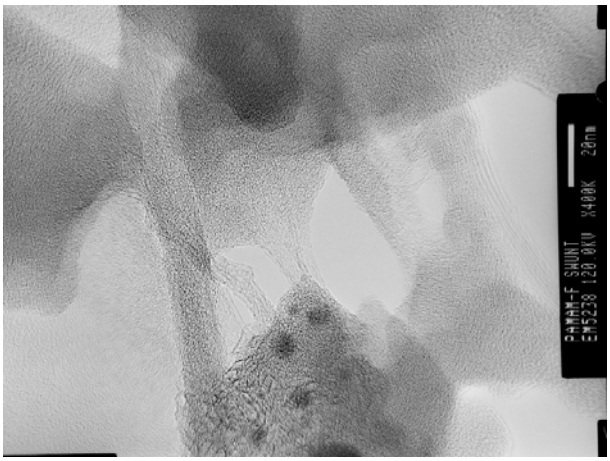

Fig. 4: TEM micrograph of the nanocomposite formed by PAMAMC + 1 wt% of SWNTs.

TEM characterization leads to the same conclusions, underlining the good affinity between the dendrimeric matrix and SWNTs. In Fig. 4, isolated and bundled nanotubes interpenetrating the dendrimer feature are well visible. Little amounts of Ni (small black drops), residual catalyst of carbon nanotube synthesis, identify the amorphous fraction of the inorganic component.

UV-VIS spectra have been performed on the samples of PAMAMC and SWNTs/PAMAMC in the wavelength range between 300 and 500 nm, where the typical signals of the dendrimer appear. Aim of this analysis has been to detect possible changes in the spectra as a consequence of nanotube increasing content. The compared spectra (Fig.5) have been normalized to the mean peak at 360 nm. The spectrum

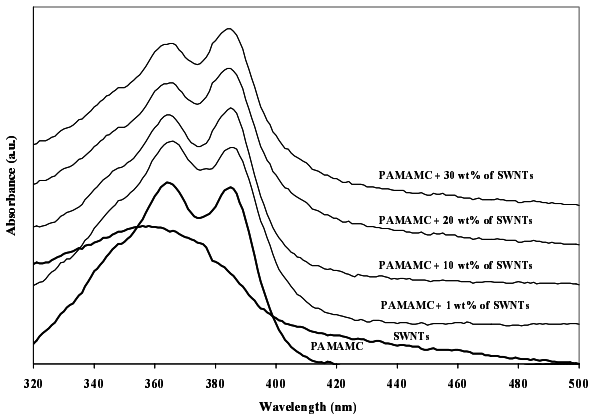

Fig. 5: UV-Vis spectra of PAMAMC, SWNTs and nanocomposites PAMAMC/SWNTs.

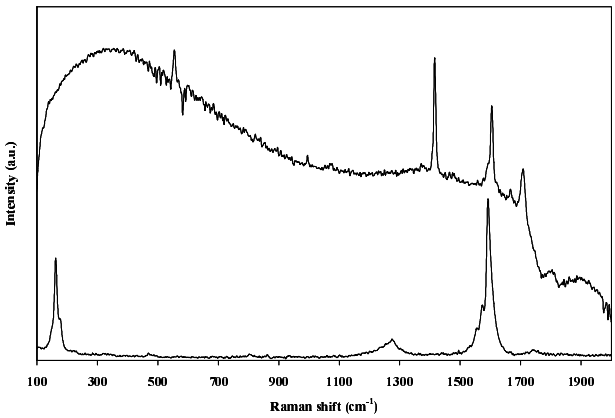

Fig. 6: Raman spectra of PAMAMC and SWNTs

of SWNTs, previously sonicated in DMF, is also reported. Going from pristine PAMAMC to composite samples, no new signal appears and the two typical peaks do not undergo any shift, although a difference in their intensity is evident. In particular, when neat PAMAMC is considered, the ratio between the first peak (360 nm) and the second peak (380 nm) is higher than unity while, when the dendrimer is combined with 10 wt% of nanotubes, it is less then unity and further decreases for the sample with 20 wt% of nanotubes. This change in the spectra is too slight to suggest modifications in the electronic structure of the dendrimer as a consequence of carbon nanotube introduction, but does not rule out the presence of weak non-covalent interactions. When the content of carbon nanotubes is high (30 wt%) no further modification in the corresponding spectrum occurs, presumably due to an excess of SWNTs not interacting with the dendrimer matrix.

Raman spectroscopy, being a powerful analytical technique to characterize SWNTs [31], has been carried out to further examine the above nanocomposites.

Usually, the SWNT spectrum is dominated by two features; in the low-frequency region (~200 cm^{-1}), there is a mode characteristic of the A_{1g} 'breathing' of the nanotube. The spectral positioning of this mode has been predicted to be essentially dependent on the diameter of the tube. In the high-frequency region (~1600 cm^{-1}), there are a number of photon modes indicative of nanotubes. These modes are due to the splitting of the optical photon, the E_{2g} mode in graphite (G-line), into longitudinal components at high energies and transverse components at lower energies. There is also a broad feature at ca. 1350 cm^{-1} (the so called D-line) that has been assigned to the presence of residual graphite and ill-organized carbon, and is found to be dependent on the excitation wavelength used.

Fig. 6 shows Raman spectra of SWNTs and PAMAMC recorded in the range between 100 and 2000 cm^{-1}. The PAMAMC spectrum does not shown relevant signals in this range if compared to the baseline noise; only the peaks at 1400 and 1600 cm^{-1}, corresponding to the aromatic C-C stretching of the naphthalendiimide groups, show a higher intensity. Precise PAMAMC peak assignment is beyond the scope of the present paper and, in any case, difficult because of the lack of references on Raman studies of PAMAMC as well as of PAMAM. Furthermore, when the spectra of the nanocomposites are considered, only SWNT signals are evident while no typical PAMAMC peak can be observed, even in the case of samples characterized by high dendrimer/nanotube ratios.

The comparison of the nanocomposite spectra shows that significant differences, as a consequence of SWNT increasing content, appear only when the radial breathing modes are considered as we previously reported [32]. In particular, an up-shift in radial bands, with respect to the corresponding values in SWNT curve, has been observed [32].

Rao et al. [33] have shown that when debundling of the nanotubes occurs, the result is an apparent up-shift in the Raman radial breathing mode frequency. This evidence is due to the fact that, for fixed laser frequency, the laser couples preferentially to isolated tubes and small bundles.

In our case, the SWNT debundling in presence of the semiconducting dendrimer is a further support of the presence of an interaction between the two components of the couple. The lack of changes in the G-band, sensitive to modification of the electron density [34], suggests an interaction of weak intensity, as deduced also from the observation of the UV-Vis spectra.

Finally, it should be noticed that the up-shift of the main radial band is noteworthy when the nanotube content is low (1 and 10 wt%), but slightly decreases for higher values, due to the presence of an excess of SWNTs interacting with PAMAMC.

The typical photoelectrical response of neat PAMAMC and PAMAMC interacting with 1 wt% of SWNT samples for the on/off light illumination cycles in air is shown in Fig. 7. The main feature in the photoelectrical temporal behaviour of interest is a fast rise/decay of the photocurrent in response to the on/off illumination step together with an enhanced decrease of resistance for the blend with SWNTs.

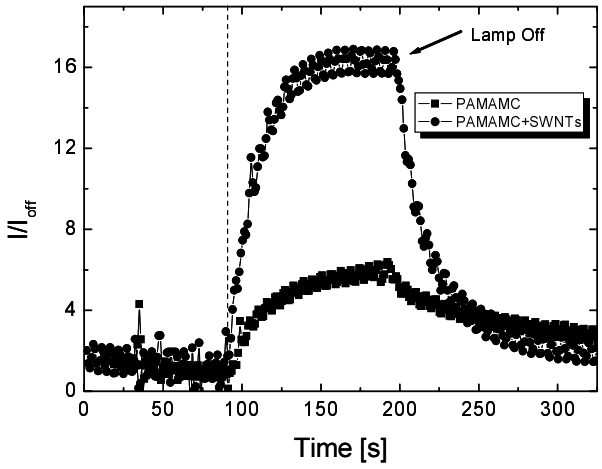

Fig. 7: Temporal photoelectrical resistance (I_{off} is the initial resistance of the sample with light off) response of PAMAMC and PAMAMC interacting with 1 wt% of SWNTs with on/off step illumination in air. At the time marked by the dashed vertical line, the sample was exposed to light.

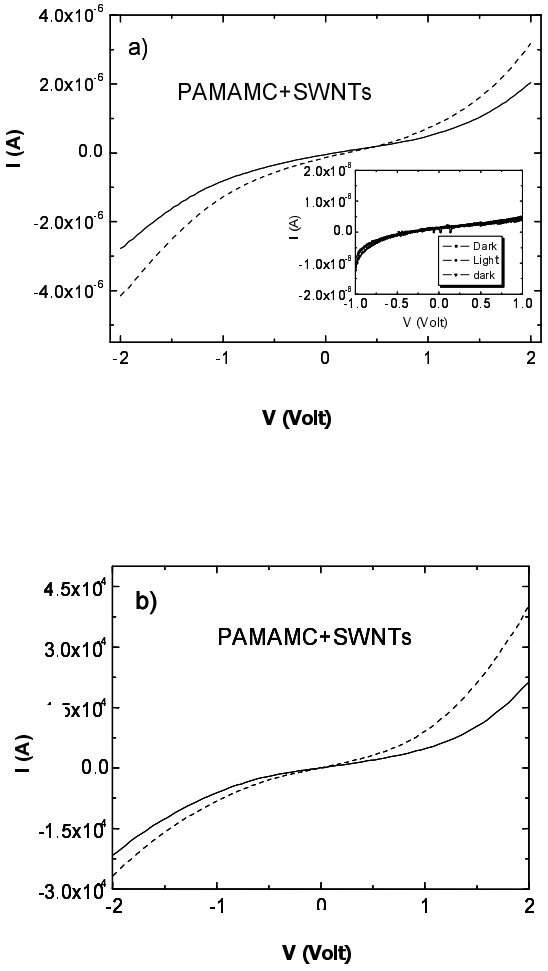

Fig. 8: I–V curves of (a) PAMAMC and (b) PAMAMC interacting with 1 wt% of SWNTs under on/off illumination steps in air (solid line sample without light, dashed line sample with light). The inset of Fig. 8 (a) shows the I-V curve of naphthalenediimide under on/off illumination steps in air.

Fig. 8a shows typical I –V curves for PAMAMC and naphthalenediimide (inset of Fig. 8a). The PAMAMC is more conductive with respect to naphthalenediimide with a photocurrent response to the on/off illumination step which is absent in the case of naphthalenediimide (see inset). Moreover the I-V curve of PAMAMC in dark is not symmetric, i.e. the absolute value of the ratio (*R*) between the current at V=±2 volts is 0.73. After the SWNT addition the current is higher than in PAMAMC and the curve, in dark, is symmetrical with *R* close to one (0.98) (Fig. 8b). The effect of SWNTs is to shift the curves to more negative biases. This behaviour is typical for the doping of a semiconductor [35,36].

It is interesting to note that during light exposure, while the *R* value for the modified PAMAM does not change (i. e. *R*=0.76 Fig. 8a), the curve for the PAMAM interacting with 1 wt% of SWNTs is no longer symmetrical, having *R*=1.5 (Fig. 8b). The finding in Fig. 8b) of a nearly flat I-V characteristics at negative biases suggests that the PAMAMC interacting with 1 wt% of SWNTs shows n-type characteristics; therefore, electron conduction can take place only at positive biases. A more appropriate evidence of the n-type behaviour needs a comparative study to be performed in thin film transistor geometry. This aspect is under investigation in our laboratories on the above new class of materials.

4. Conclusions

A new nanocomposite system has been prepared combining carbon nanotubes with a semiconducting dendrimer characterized by highly aromatic end groups. Non-covalent interactions between PAMAMC and single-walled carbon nanotubes have been promoted by sonication in DMF. SEM and TEM microscopies, performed in order to study the level of dispersion of the inorganic filler in the organic matrix, confirm the formation of a nanocomposite material.

UV-Vis and Raman spectroscopy have been useful for establishing the intensity of the interactions that favoured an intimate mixing of the two elements. UV-Vis spectroscopy, with respect to modifications of PAMAMC structure, and Raman spectroscopy, as regards modifications of nanotube structure, have shown that the aforementioned interactions occur but are weak. Indeed, no modification of the electronic structure has been evidenced.

Acknowledgements

Dr. Mauro Michetti and Mr. Claudio Uliana for SEM and TEM analyses and Dr. Davide Comoretto for many helpful discussions are gratefully acknowledged. The present research has been supported by PRIN MIUR funds (2003093440). The authors acknowledge the support of NoE 'Nanofun-Poly' for the diffusion of the research results.

References:

1. **Iijima, S.,** "Helical microtubules of graphitic carbon", *Nature*, **354** (1991), 56-58.

2. **Harris**, **P.J.F.,** "Carbon nanotubes and related structures", *Cambridge University Press*, *Cambridge*, 1999.

3. **Tanaka, K., Yamabe, T.,** and **Fukui K.,** (Eds.), "The science and technology of carbon nanotubes", *Elsevier, Oxford*, 1999.

4. **Avouris, P., Dresselhaus, G.,** and **Dresselhaus M.S.** (Eds.), "Carbon nanotubes synthesis, structure, properties and applications", *Spriger*, *Berlin*, 2000.

5. **Dresselhaus, M.S., Dresselhaus G.,** and **Eklund**, **P.C.,** "Science of fullerenes and carbon nanotubes", *Academic Press*, *San Diego*, 1996.

6. **Dekker, C.** ,"Carbon nanotubes as molecular quantum wires", *Phys. Today*, **52** (1999), 22-28.

7. **Dai, H.**, "Controlling nanotube growth", *Phys. World*, **13** (2000), 43-47.

8. **Bahr, J.L., Yang, J., Kosynkin, D.V., Bronikowski, M.J., Smalley, R.E.,** and **Tour, J. M.,** "Functionalization of carbon nanotubes by electrochemical reduction of aryl diazonium salts: a bucky paper electrode", *J. Am. Chem. Soc.*, **123** (2001), 6536-6542.

9. **Holzinger, M., Vostrowsky, O., Hirsch, A., Hennrich, F., Kappes, M., Weiss, R.,** and **Jellen, F.,** "Sidewall functionalization of carbon nanotubes", *Angew. Chem., Int. Ed.*, **40** (2001), 4002-4005.

10. **Georgakilas, V., Kordatos, K., Prato, M., Guldi, D. M., Holzinger, M.,** and **Hirsch, A.,** "Organic functionalization of carbon nanotubes", *J. Am. Chem. Soc.*, **124** (2002), 760-761.

11. **Mickelson, E.T., Huffman, C.B., Rinzler, A.G., Smalley, R.E., Hauge, R.H.,** and **Margrave, J.L.,** "Fluorination of SWCNT", *Chem. Phys. Lett.*, **296** (1998), 188-194.

12. **Murakami, H., Nomura, T.,** and **Nakashima, N.,** "Noncovalent porphyrin-functionalized single-walled carbon nanotubes in solution and the separation of porphyrin-nanotube nanocomposite", *Chem. Phys. Lett.*, **378** (2003), 481–485.

13. **Nakashima, N., Tomonari, Y.,** and **Murakami, H.,** "Water-soluble single-walled carbon nanotubes via noncovalent sidewall-functionalization with a pyrene-carrying ammonium ion", *Chem. Lett.*, (2002), 638-639.

14. **Nakashima, N., Okuzono, S., Murakami, H., Nakai, T.,** and **Yosihkawa, K.,** "DNA dissolves single-walled carbon nanotubes in water", *Chem. Lett.,* **32** (2003), 456-457.

15. **Krstic, V., Duesberg, G.S., Muster, J., Burghard, M.,** and **Roth, S.**, "Langmuir-Blodgett films of matrix-diluted single-walled carbon nanotubes", *Chem. Mater.*, **10** (1998), 2338-2340.

16. **Nakashima, N., Kobae, H., Sagara, T.,** and **Murakami, H.,** "Formation of single-walled carbon nanotube thin films on electrodes monitored by an electrochemical quartz crystal microbalance", *Chem. Phys. Chem.*, **3** (2002), 456-458.

17. **O'Connel, M.J., Boul, P., Ericson, L.M., Huffman, C., Wang, Y., Haroz, E., Kuper, C., Tour, J., Ausman, K.D.,** and **Smalley, R.E.,** "Reversible water-solubilization of single-walled carbon nanotubes by polymer wrapping", *Chem. Phys. Lett.*, **342** (2001), 265-271.

18. **Star, A., Stoddart, J.F., Steuerman, D., Diehl, M., Boukai, A., Wong, E.W., Yang, X., Chung, S.-W., Choi, H.,** and **Heath, J.R.,** "Preparation and properties of polymer-wrapped single-walled carbon nanotubes", *Angew. Chem. Int. Ed.*, **40** (2001), 1721-1725.

19. **Chen, J., Liu, H., Weimer, W.A., Halls, M.D., Waldeck, D.H.,** and **Walker, G.C.,** "Noncovalent engineering of carbon nanotube surfaces by rigid, functional conjugated polymers", *J. Am. Chem. Soc.*, **124** (2002), 9034-9035.

20. **Steuerman, D.W., Star, A., Narizzano, R., Choi, H., Roes, R.S., Nicolini, C., Stoddart, J.F.,** and **Heath, J.R.,** "Interactions between conjugated polymers and single-walled carbon nanotubes", *J. Phys. Chem. B*, **106** (2002), 3124-3130.

21. **Huang, J., Li, X.H., Xu, J.C.,** and **Li, H.L.,** "Well-dispersed single-walled carbon nanotube/polyaniline composite films", *Carbon*, **41** (2003), 2731–2736.

22. **Chen, R. J., Zhang, Y., Wang, D.,** and **Dai, H.,** "Non-covalent sidewall functionalization of single-walled carbon nanotubes for protein immobilization", *J. Am. Chem. Soc.*, **123** (2001), 3838-3839.

23. **Dalton, A. B., Stephan, C., Coleman, J. N., McCarthy, B., Ajayan, P. M., Lefrant, S., Bernier, P. Blau, W. J.,** and **Byrne, H. J.,** "Selective interaction of a semi-conjugated polymer with single wall nanotubes", *J. Phys. Chem. B*, **104** (2000), 10012-10016.

24. **Star, A., Liu, Y., Grant, K., Ridvan, L., Stoddart, J. F., Steuerman, D.W., Diehl, M.R., Boukai,** and **A., Heath, J.R.,** "Noncovalent side-wall functionalization of single-walled carbon nanotubes", *Macromolecules*, **36** (2003), 553-560.

25. **Zhang, J., Lee, J.K., Wu, Y.,** and **Murray, R.W.,** "Photoluminescence and electronic interaction of anthracene derivatives adsorbed on sidewalls of single-walled carbon nanotubes", *Nano Lett.*, **3** (2003), 403-407.

26. **Niyogi, R., Hamon, M.A.,** and **Haddon, R.C.,** "Chemistry of single-walled carbon nanotubes", *Acc. Chem. Res.*, **35** (2002), 1105–1113.

27. **Tabakovic, I., Miller, L.L., Duan, R.G., Tully, D.,** and **Tomalia, D.A.,** "Dendrimers peripherally modified with anion radicals that form π-dimers and π-stacks", *Chem. Mater.*, **9** (1997), 736- 745.

28. **Ausman, K.D., Piner, R., Lourie, O., Ruoff, R.S.,** and **Korobov, M.,** "Toward solutions of pristine nanotubes", *J. Phys. Chem. B*, **104** (2000), 8911 - 8915.

29. **Chen, J., Rao, A.M., Lyuksyutov, S., Itkis, M.E., Hamon, M.A., Hu, H., Cohn, R.W., Eklund, P.C., Colbert, D.T., Smalley, R.E.,** and **Haddon, R.C.,** "Dissolution of full-length single-walled carbon nanotubes", *J. Phys. Chem. B*, **105** (2001), 2525 - 2528.

30. Kimizuka, N., Kawasaki, T., Hirata, K., and **Kunitake, T.**, "Tube-like nanostructures composed of networks of complementary hydrogen bonds", *J. Am. Chem. Soc.*, **117** (1995), 6360-6361.

31.. **Duesberg, G.S, Blau, W.J., Byrne, H.J., Muster, J., Burghard, M.,** and **Roth, S.,** "Experimental observation of individual single-wall nanotube species by Raman microscopy", *Chem. Phys. Lett.*, **310** (1999), 8-14.

32. Valentini, L., Armentano, I., Ricco, L., Alongi, J., Pennelli, G., Mariani, A., Russo, S., and **Kenny, J.M.,** "Selective Interaction of Single-Walled Carbon Nanotubes with Conducting Dendrimer", *Diamond and Related Materials*, (in press; doi:10.1016/j.diamond.2005.07.003)

33. Rao, A.M., Chen, J., Ritchter, E., Schlecht, U., Eklund, P.C., Haddon, R.C., Venkateswaran, U.D., Known, Y.K., and **Tomanek, D.,** "Effect of van der Waals interactions on the Raman modes in single walled carbon nanotubes", *Phys. Rev. Lett.*, **86** (2001), 3895-3898.

34. Wise, K.E., Park, C., Siochi, E.J., and **Harrison, J.S.,** "Stable dispersion of single wall carbon nanotubes in polyimide: the role of noncovalent interactions", *Chem. Phys. Lett.*, **391** (2004), 207-211.

35. **Ozel, T., Gaur, A., Rogers, J.A.,** and **Shim, M.,** "Polymer electrolyte gating of carbon nanotube network transistors", *Nano Lett.*, **5** (2005), 905-911.

36. Zhou, Y.X., Gaur, A., Hur, S.H., Kocabas, C., Meitl, M.A., Shim, M., and **Rogers, J.A.,** "p-channel, n-channel thin film transistors and p-n diodes based on single wall carbon nanotube networks", *Nano Lett.*, **4** (2004), 2031-2035.